Denoising Technique Using Double Density Dual Tree DWT for Medical Images

Dr.B. Shoban Babu[1*], Dr.S. Swarnalatha[2], Dr.V. Govindaraj[3]

[1*]Professor, Department of ECE, Sri Venkateswara College of Engineering, Tirupati, A.P, India.

[2]Professor, Department of ECE, Sri Venkateswara University College of Engineering, Tirupati, A.P, India.

[3]Assistant Professor, Department of ECE, Dr.NGP Institute of Technology, Coimbatore, Tamil Nadu, India.

Abstract

Even with several techniques or algorithms for denoising implemented, image denoising remains a difficult subject for academics. The implementation of the picture denoising algorithm utilising Double Density Dual Tree Wavelet Transforms is covered in this paper, along with a discussion of critical sampling (Discrete Wavelet) and over complete sampling (Double Density Wavelet) based wavelet transforms. The picture denoising results lead to a few key conclusions, including the fact that complicated wavelet transforms do not always outperform real discrete wavelet transforms and that it is not always true that more redundancy equals higher image denoising performance.

Index Terms: DWT, Medical Images, Denoising, Artefacts.

DOI: 10.47750/pnr.2022.13.S03.262

INTRODUCTION

Images must be denoised before being processed for computer vision and other modern applications, such as medical imaging. This is a crucial step in image processing and analysis. Denoising's objective is to eliminate noise. Better spatial and spectral localization of image generation is provided by the Discrete Wavelet Transform (DWT) of images, which generates a non-redundant picture representation [1]. The DWT has two significant issues:

- Lack of shift invariance: This is the outcome of each level's down sampling process. The wavelet coefficients' amplitude varies significantly when the input signal is gently shifted.
- Lack of directional selectivity: Due to the actual and separable nature of the DWT filters, the DWT is unable to differentiate between the opposing diagonal directions.

These disadvantages might be lessened by a sophisticated wavelet transform. Kingsbury's dual-tree version of the CWT (DT-CWT), which is suggested [2], uses two trees with real filters to independently create the real and imaginary sections of the wavelet coefficients. With the DT-CWT, which is an alternative to the standard DWT, the aliased components of the signal are suppressed, approximate shift invariance is attained, and the outputs of each tree are down sampled by adding the outputs of the two trees during reconstruction. Compared to the separable DWT, the DT-CWT has better shift-invariance and directional selectivity [3].

Double density wavelet transform is yet another variety of complex wavelet transform. The double density DWT is developed using the three-channel filter. In comparison to an orthonormal wavelet basis, the double density DWT is less shift-sensitive and has less rectangular artefacts. The complicated double density dual tree wavelet transform is a discrete wavelet transform that is overly full and created to have both the characteristics of a dual tree complex wavelet transform and a double density discrete wavelet transform. The dual tree CWT and the double density DWT are substantially dissimilar from one another in some crucial ways, such as the fact that they are both over complete by a factor of two, almost shift-invariant, and based on FIR perfect reconstruction filter banks. For a number of signal processing applications, both wavelet transforms can outperform the critically sampled DWT [4], but they do so at a higher cost.

DOUBLE DENSITY DWT

The double density DWT features less rectangular artefacts and is less shift-sensitive than an orthonormal wavelet basis. A discrete wavelet transform that is excessively full and designed to have traits of both a dual tree complex wavelet transform and a double density discrete wavelet transform is known as a complicated double density dual tree wavelet transform. In several essential ways, such as the fact that they are both over complete by a factor of two, nearly shift-invariant, and built on FIR perfect reconstruction filter banks, the dual tree CWT and the double density DWT are significantly different from one another. Both wavelet transforms can outperform the critically sampled DWT for a variety of signal processing applications, but they do so at a

higher cost.

The double density DWT is an improvement on the critically sampled DWT and provides a denser sampling of the time-frequency plane with crucial additional properties: (i) It uses two separate wavelets that are intended to be offset from one another by half, together with one scaling function. (ii) The double-density DWT is two times over complete. It is almost shift-invariant (iii). In terms of denoising, this transform outperforms the conventional DWT in two dimensions.

To construct a Double Density DWT with FIR filters we use the oversampled filter bank [5]. The filter $h_o(n)$ is a LPF (scaling) while $h_1(n)$and $h_2(n)$ are HPFs (wavelet) as shown in fig.1. The three-channel filter bank which we use to develop the Double Density DWT corresponds to a wavelet frame based on a single scaling function $\emptyset(t)(1)$ and two distinct wavelets $\psi_1(t)$ and $\psi_2(t)$ (2).

$$\emptyset(\boldsymbol{t}) = \sqrt{\boldsymbol{2}} \sum_{\boldsymbol{n}} \boldsymbol{h_o}\,(\boldsymbol{n})\emptyset(\boldsymbol{2t} - \boldsymbol{n}) \ldots\ldots\ldots\ldots\ldots\ldots\ldots\ldots\ldots\ldots (\boldsymbol{1})$$

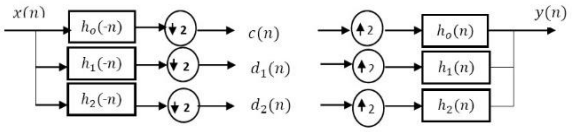

Fig. 1. 3-Channel Perfect Reconstruction Filter Bank

$$\boldsymbol{\psi_i(t)} = \sqrt{\boldsymbol{2}} \sum_{\boldsymbol{n}} \boldsymbol{h_i}\,(\boldsymbol{n})\emptyset(\boldsymbol{2t} - \boldsymbol{n})\ \boldsymbol{i} = \ \boldsymbol{1, 2} \ldots\ldots\ldots\ (\boldsymbol{2})$$

The *analysis filter bank* consists of three analysis filters: *one low pass filter* denoted by $h_o(-n)$ and *two distinct high pass filters* denoted by $h_1(-n)$ and $h_2(-n)$ As the input signal *x(n)* travels through the system, the analysis filter bank decomposes it into three sub-bands, each of which is then down-sampled by 2. From this process the signals $c(n), d_1(n), and\ d_2(n)$are obtained which represent the low frequency sub-band, and the two high frequency (detail) sub-bands respectively.

The *synthesis filter bank* consists of three synthesis filters: *one low pass filter* denoted by $h_o(n)$and *two distinct high pass filters* denoted by $h_1(n)$and $h_2(n)$ which are essentially the inverse of the analysis filters.As the three sub-band signals travel through the system, they are up-sampled by two, filtered, and then combined to form the output signal $y(n)$. One of the main concerns in filter bank design is to ensure the Perfect Reconstruction (PR) condition i.e. $y(n) = x(n)$.

A. 1-D Double-Density DWT

The double-density DWT is implemented by recursively applying the 3-channel analysis filter bank to the low pass subband. This process is illustrated in fig. 2. Conversely, the inverse double-density DWT is obtained by iteratively applying the synthesis filter bank.

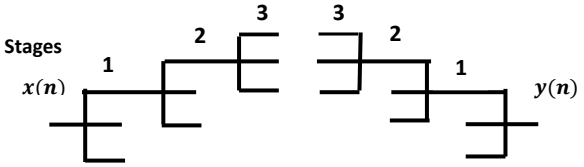

Fig. 2. Three Level Decomposition and Reconstruction of 1D-DDDWT

B. 2-D Double-Density DWT

We need to put into practise a 2-D analysis and synthesis filter bank structure in order to handle 2-D signals and images using the double-density discrete wavelet transform [6]. This is easily accomplished by applying the transform alternately to an image's rows and columns first. As illustrated in Fig. 3, this results in nine 2-D sub-bands, of which one is the 2-D low pass scaling filter and the other eight are the eight 2-D wavelet filters.

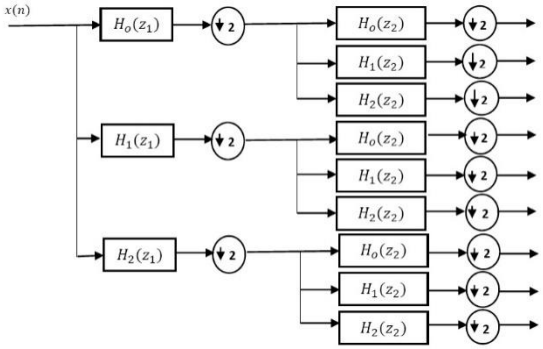

Fig. 3. Analysis Filter Bank representation of 2D- DDDWT

DOUBLE DENSITY DUAL TREE DWT

We suggested the Double-Density Dual-Tree Discrete Wavelet Transform (DDDTDWT), which combines the benefits of both the Dual-Tree CWT and the Double-Density DWT. The Double-Density DWT and the Dual-Tree CWT are comparable in a number of ways (they are both two times over complete, essentially shift-invariant, and based on FIR perfect reconstruction filter banks), but they differ significantly in other crucial ways. For a variety of signal processing applications, both wavelet transforms can surpass the critically sampled DWT, albeit for various reasons. Therefore, it is likely to look into the possibility of a single wavelet transform that combines the traits of the Dual-Tree Complex DWT and Double-Density DWT [7-8]. The motivation is as follows.

The Dual-Tree DWT is based on two unique scaling functions and four distinct wavelets, two of which are offset from one another by half in the first pair and two of which roughly correspond to the Hilbert transform pair in the second pair. In order for the integer translates of one wavelet pair to fall in the middle of the integer translates of the other pair, the first pair of the four wavelets are intended to be offset from the other pair. In order to create two

complicated (roughly analytical) wavelets, the second pair of the four wavelets is made to approximate Hilbert transform the other pair of wavelets. In order to implement sophisticated and directed wavelet transforms, they can be used.

In order to implement sophisticated and directed wavelet transforms, they can be used. The paraunitary filter bank completion and flat-delay filter spectral factorization provide the foundation of the design process for the Double-Density Dual-Tree CWT. The solutions have compact support and vanishing moments. In contrast to Dual-Tree wavelets and unlike Double-Density wavelets, the generated wavelets produce approximative Hilbert transform pairs [9]. The degree to which the approximation is satisfied is also determined by a parameter L in the design procedure.

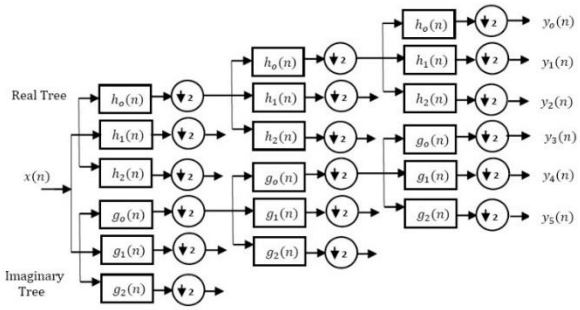

Fig. 4. Iterated filter bank for the Double-Density Dual-Tree DWT

The Double-Density Dual-Tree DWT [10] proposed is based on concatenating two oversampled DWTs, it's filter bank structure consists of two oversampled iterated filter banks operating in parallel similar to the Dual-Tree DWT. The oversampled filter bank is illustrated in Fig. 4. The iterated oversampled filter bank corresponding to the implementation of the Double-Density Dual-Tree is illustrated in fig. 5. Let us denote the filters the first filter bank by $h_i(n)$ and the filters in the second filter bank by $g_i(n)$for i = 0,1,2. In each of the filter banks, the synthesis filters are the time-reversed versions of the analysis filters. The goal is to design the 6-FIR filters that satisfy,

1. The perfect reconstruction property.
2. The wavelets form two Hilbert transform pairs.
3. The wavelets have specified vanishing moments.

Using the infinite product formula, it was shown that for two orthogonal wavelets to form a Hilbert transform pair, the scaling filters should be offset by a half sample. In that, a design problem was formulated for the minimal length scaling filters such that the wavelets each have a specified number of vanishing moments K and the half-sample delay approximation is flat at $w = 0$ with specified degree L. The low pass filters $\boldsymbol{h_o(n)}, \boldsymbol{g_o(n)}$fully determine the two orthogonal wavelet bases. We look for pairs of orthonormal wavelets where the low pass scaling filters have the form,

$$h_o(n) = f(n) * d(n) \dots\dots\dots\dots\dots\dots\dots\dots\dots\dots\dots\dots\dots\dots (3)$$

$$g_o(n) = f(n) * d(L-n) \dots\dots\dots\dots\dots\dots\dots\dots\dots\dots\dots\dots\dots\dots (4)$$

In terms of the transfer functions, we have

$$H_o(z) = F(z)D(z) \dots\dots\dots\dots\dots\dots\dots\dots\dots\dots\dots\dots\dots\dots (5)$$

$$G_o(z) = F(z)z^{-L}D\left(1/z\right) \dots\dots\dots\dots\dots\dots\dots\dots\dots\dots\dots\dots (6)$$

$$G_o(z) = H_0(z)\frac{z^{-L}D\left(1/z\right)}{D(z)} \dots\dots\dots\dots\dots\dots\dots\dots\dots\dots (7)$$

The design procedure depends on the design of an All-pass filter with approximately constant fractional delay. Several authors have addressed the design of All Pass systems that approximate a fractional delay the following formula for the maximally flat delay. All Pass filter is adapted from Thiran's formula for the maximally flat delay all pole filter. We can recognize that the transfer functions. The maximally flat approximation to a delay of τ samples,

$$A(z) = \frac{z^{-L}D\left(1/z\right)}{D(z)} \dots\dots\dots\dots\dots\dots\dots\dots\dots\dots\dots\dots (8)$$

The maximally flat type, which is accurate with a degree of tangency L at $w = 0$, is an all pass system with $A(w) = 1$. (9-11) and all Pass system $A(z)$ is an approximate half sample delay (12-13).

$$D(z) = 1 + \sum_{n=1}^{L} d(n)\, z^{-n} \dots\dots\dots\dots\dots\dots\dots\dots\dots (9)$$

$$d(n) = (-1)^n \binom{L}{n} \frac{(r-L)n}{(r+1)n} \dots\dots\dots\dots\dots\dots\dots (10)$$

$$|G_o(w)| = |H_0(w)|, |G_1(w)| = |H_1(w)| \; and \; |\psi_g(w)| = |\psi_h(w)| \dots (11)$$

$$A(w) \approx e^{-jw/2} \; around \; w = 0 \dots\dots\dots\dots\dots\dots (12)$$

$$A(z) \approx z^{-\frac{1}{2}} \; around \; z = 1 \dots\dots\dots\dots\dots\dots (13)$$

If the $\boldsymbol{H_0(w)}$and $\boldsymbol{G_o(w)}$are low pass CQF filters with (14) Then the corresponding wavelets are the Hilbert transform pair (15),

$$G_o(w) = H_0(w)e^{-jw/2} \; for |w| < \pi \dots\dots\dots (14)$$

$$\psi_g(t) = H\{\psi_h(t)\} \dots\dots\dots\dots\dots\dots\dots\dots\dots\dots (15)$$

The parallel combination of two DWTs designed to satisfy (15)is called the dual-tree complex DWT [11] equivalently, digital filter $\boldsymbol{g_o(n)}$ is a half sample delay version of $\boldsymbol{h_o(n)}$**(16)**.

$$g_o(n) = h_o(n - 1/2) \dots\dots\dots\dots\dots\dots\dots\dots\dots\dots (16)$$

This paper highlights wavelet based enhancement of grayscale digital images corrupted by Additive White Gaussian Noise. The Double Density Dual Tree Discrete Wavelet Transform outperforms in comparison with others wavelet transform in the highly corrupted images. In terms of image enhancement, the Double-Density complex wavelet transform performed much better by suppressing noise over the Double-Density discrete wavelet transform. However, to improve the performance further it is necessary to use a different threshold for each sub-band because for this transform the wavelets associated with different sub-bands have different norms. The simulation results indicate that the Complex Double Density Dual Tree DWT performances better than others wavelet transform.

IMAGE DENOISING

Noise is a colloquial term for an unpleasant, intolerable, and unwelcome sound. An undesired disturbance to a desired signal is referred to as noise in both analogue and digital image processing languages. When working with data from real-world signals in 1-D (pictures in 2-D), applied scientists, engineers, and academics must account for noise. Regardless of the frequency content of the image, image denoising aims to eliminate any noise (high frequencies or low frequencies) existing in the image while preserving its original content. The original signal (time-space) domain and the transform domain are the two possible domains for image denoising. There are two approaches to image denoising in turn.

In this paper ***image denoising is accomplished in time-scale domain via wavelet transform by thresholding the detailed wavelet coefficients of the Double Density Wavelet Decompositions of the image effected with Additive White Gaussian Noise (AWGN).*** The two major types of wavelet coefficients thresholding techniques are.

A. Soft Thresholding

The soft thresholding filter is non-parametric filterused to put to zero all the wavelet coefficients with the absolute value smaller than a threshold. This threshold is selected to minimize the min-max approximation error. The I/P-O/P relation of the soft thresholding function (17),

$$\widehat{w_s}(w_x) = \begin{Bmatrix} w_x - t & for\ |w_x| > t \\ o & for\ |w_x| \le t \\ w_x + t & for\ |w_x| < -t \end{Bmatrix} \dots\dots\dots\dots\dots (17)$$

B. Hard Thresholding

Another type of non-parametric filter is the hard-thresholding filter. This is also a shrinkage operator. The$i/p - o/p$ relation of the hard thresholding function (18),

$$\widehat{w_h}(w_x) = \begin{Bmatrix} w_x for |w_x| \ge t \\ o for |w_x| < t \end{Bmatrix} \dots\dots\dots\dots\dots\dots\dots (18)$$

Where$w_x = w_s + w_n$and t is a threshold, w_x represents the sequence of wavelet coefficients of the noisy image, w_s *and* w_n represents the sequence of the wavelet coefficients of the noiseless component and noise component respectively.

The performance of this denoising algorithm is graded by two error metrics, one is Mean Square Error and another one is Peak Signal to Noise Ratio.

The Mean Square Error (MSE) is calculated by (12),

$$MSE = \frac{1}{MN}\sum_{y=1}^{N}\sum_{x=1}^{M}[f(x,y) - f_0(x,y)]^2 \dots\dots\dots\dots (12)$$

Where $f(x,y)$ is the input image, $f_0(x,y)$is the output image, may be noisy or denoised, M and N are the number of rows and columns of the image, respectively. ***The smaller the MSE, the better the denoising.***

The Peak Signal to Noise Ratio (PSNR) is computed by (13),

$$PSNR = 10log_{10}\left(\frac{R^2}{MSE}\right) \dots\dots\dots\dots\dots\dots\dots\dots\dots\dots (13)$$

Where *R* is the maximum value in the input image data type. If the pixels of the digital image is represented using ***n bits***, then $R = 2^n - 1$. In this paper we have considered grey scale digital images that are represented using *8 bits*, *i.e.* $R = 2^8 - 1 = 255$. ***The larger the PSNR, the better the denoising***.

RESULTS AND DISCUSSION

The performance of the Double Density Wavelet Transforms and Complex Double Density Dual Tree Wavelet Transforms is examined for the images ***Lena*** and ***Stonehenge***. Each of the images is corrupted with AWGN standard deviations in the range of 10 to 100 in steps of 10. The noisy images are subjected to Double Density Discrete Wavelet Transform (DDDWT), Double Density Dual Tree Wavelet Transform (DDDTDWT) and Double Density Dual Tree Complex Wavelet Transform (DDDTCWT) to obtain the approximation and detailed wavelet coefficients. The soft Thresholding technique is applied over the detailed wavelet coefficients by considering the different threshold values in the range of 10 to 100 in steps of 10. The filtered wavelet coefficients are subjected to the inverse wavelet transform to obtain the denoised image respectively.

(i) Original Image (Lena 512 x 512)

(ii) Noisy Image (Lena 512 x 512)

(iii) Denoised using DDDWT (MSE=77.95778, PSNR=29.2122)

(iv) Denoised using DDDTDWT (MSE=80.10478, PSNR=29.09422)

(v) Denoised using DDDTCWT (MSE=81.66655, PSNR=29.01036)

Fig. 7(a). Represents (i) Original Image, (ii) the noisy image and (iii) to (v) denoised images obtained using DDDWT, DDDTDWT and DDDTCWT techniques respectively with ($\boldsymbol{\sigma}$ = **20**) for Lena 512 x 512 image.

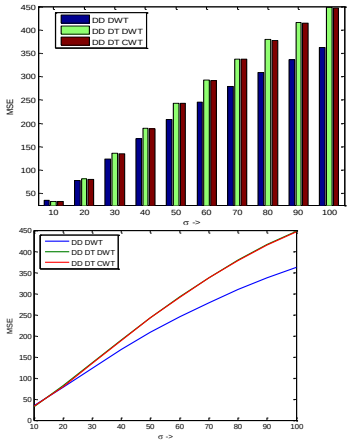

Fig. 7(b). Variation of MSE of different image denoising techniques for different values of σ for Lena 512 x 512 image.

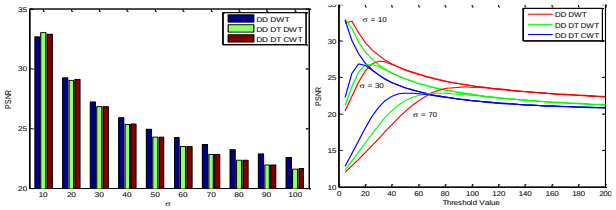

Fig. 7(c). Variation of PSNR of different image denoising techniques for different values of σ for Lena 512 x 512 image.

Table 1(a). Comparison of MSE values of the DDDWT, DDDTDWT, and DDDTCWT image denoising Techniques for Lena 512 x 512 image

$\sigma \rightarrow$ / ***WAVELETS***	**10**	**20**	**30**	**40**	**50**
DDDWT	**35.13**	**77.96**	**123.66**	**167.62**	**208.40**
DDDTDWT	**32.65**	**81.67**	**135.75**	**189.75**	**242.95**
DDDTCWT	**33.64**	**80.10**	**134.87**	**189.02**	**243.18**
$\sigma \rightarrow$ / ***WAVELETS***	**60**	**70**	**80**	**90**	**100**
DDDWT	**245.43**	**278.71**	**309.35**	**336.90**	**361.98**
DDDTDWT	**292.32**	**337.99**	**379.34**	**415.93**	**448.21**
DDDTCWT	**291.63**	**337.31**	**377.64**	**414.63**	**447.19**

Table 1(b). Comparison of PSNR values of the DDDWT, DDDTDWT, and DDDTCWT image denoising Techniques for Lena 512 x 512 image

$\sigma \rightarrow$ / ***WAVELETS*** ↓	10	20	30	40	50
DDDWT	**32.67**	**29.21**	**27.21**	**25.89**	**24.94**
DDDTDWT	**32.99**	**29.01**	**26.80**	**25.35**	**24.28**
DDDTCWT	**32.86**	**29.09**	**26.83**	**25.37**	**24.28**
$\sigma \rightarrow$ / ***WAVELETS*** ↓	60	70	80	90	100
DDDWT	**24.23**	**23.68**	**23.23**	**22.86**	**22.54**
DDDTDWT	**23.47**	**22.84**	**22.34**	**21.94**	**21.62**
DDDTCWT	**23.48**	**22.85**	**22.36**	**21.95**	**21.63**

A. Observations from figure 7 and table 1

Table 2(b). Comparison of PSNR values of the DDDWT, DDDTDWT, and DDDTCWT image denoising Techniques for Stonehenge512 x 512 image

$\sigma \rightarrow$ / ***WAVELETS*** ↓	10	20	30	40	50
DDDWT	**33.99**	**30.46**	**28.43**	**27.10**	**26.13**
DDDTDWT	**33.67**	**30.03**	**27.93**	**26.50**	**25.48**
DDDTCWT	**33.83**	**30.08**	**27.94**	**26.57**	**25.54**
$\sigma \rightarrow$ / ***WAVELETS*** ↓	60	70	80	90	100
DDDWT	**25.38**	**24.77**	**24.27**	**23.85**	**23.49**
DDDTDWT	**24.65**	**23.98**	**23.42**	**22.95**	**22.56**
DDDTCWT	**24.71**	**24.04**	**23.48**	**23.01**	**22.62**

Fig 7(a) represents Original Image, noisy image and denoised images obtained using DDDWT, DDDTDWT and DDDTCWT image denoising techniques with (σ=20) for Lena 512 x 512 image. Fig 7(b) Variation of MSE of different image denoising techniques for different values of σ for Lena 512 x 512 image using bar graph and line plot. Fig 7(c). Variation of PSNR of different techniques for different values of σ for Lena 512 x 512 image using bar graphs and line plots for easier interpretation. Table 1(a) and 1(b) shows comparison of MSE and PSNR values of the DDDWT, DDDTDWT, and DDDTCWT Techniques for image denoising using Lena image 512 x 512 respectively.

(i) Original Image (Stonehenge 512 x 512)

(ii) Noisy Image (Stonehenge 512 x 512)

(iii) Denoised using DDDWT (MSE=77.957, PSNR=29.212)

(iv) Denoised using DDDTDWT (MSE=80.105, PSNR=29.094)

(v) Denoised using DDDTCWT (MSE=81.666, PSNR=29.011)

Fig. 8(a). Represents (i) Original Image, (ii) the noisy image and (iii) to (v) denoised images obtained using DDDWT, DDDTDWT and DDDTCWT techniques respectively with ($\sigma = 20$) for Stonehenge512 x 512 image.

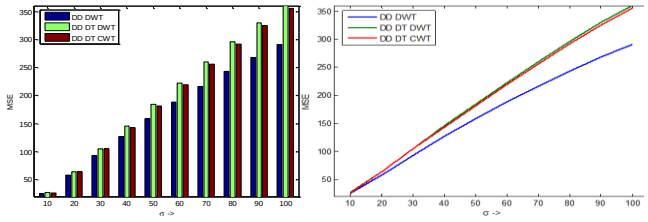

Fig. 8(b). Variation of MSE of different image denoising techniques for different values of σ for Stonehenge 512 x 512 image

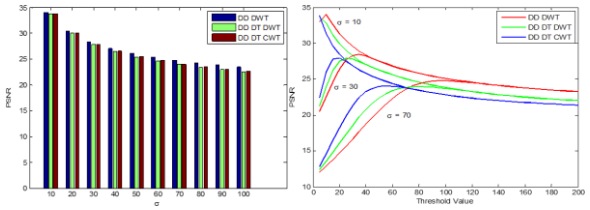

Fig. 8(c). Variation of PSNR of different image denoising techniques for different values of σ for Stonehenge512 x 512 image.

Table 2(a). Comparison of MSE values of the DDDWT, DDDTDWT, and DDDTCWT image denoising Techniques for Stonehenge 512 x 512 image

σ → ***WAVELETS***	**10**	**20**	**30**	**40**	**50**
DDDWT	**25.94**	**58.45**	**93.26**	**126.81**	**158.47**
DDDTDWT	**27.92**	**64.55**	**104.78**	**145.46**	**184.25**
DDDTCWT	**26.90**	**63.90**	**104.60**	**143.25**	**181.56**
σ → ***WAVELETS***	**60**	**70**	**80**	**90**	**100**
DDDWT	**188.38**	**216.79**	**243.01**	**267.75**	**291.02**
DDDTDWT	**222.78**	**260.22**	**295.95**	**329.60**	**360.36**
DDDTCWT	**219.59**	**256.44**	**291.74**	**324.88**	**355.41**

B. Observations from Figure 8 and Table 2

Fig 8(a) represents Original Image, noisy image and denoised images obtained using DDDWT, DDDTDWT and DDDTCWT image denoising techniques with (σ=20) for Stonehenge image512 x 512 image. Fig 8(b). Variation of MSE of different image denoising techniques for different values of σ Stonehenge image 512 x 512 image using bar graph and line plot. Fig 8(c).Variation of PSNR of different techniques for different values of σ for Stonehenge image512 x 512 image using bar graphs and line plots for easier interpretation. Table 2(a) and 2(b) shows comparison of MSE and PSNR values of the DDDWT, DDDTDWT, and DDDTCWT Techniques for image denoising using Stonehenge image 512 x 512 respectively.

CONCLUSION

In this paper implementation of image denoising technique is carried out by three Double Density Wavelet Transforms DDDWT, DDDTDWT and DDDTCWT. The image denoising capability of these techniques is analyzed by selecting AWGN and by setting different threshold values. From section V it is observed (a) The DDDTCWT performs well at low levels of noise. However, Double Density Discrete Wavelet Transform suits well for high levels of noise. (b) The DDDTCWT based image denoising technique is better than the rest of the two techniques, at low values of Threshold values, irrespective of the noise level. (c) The PSNR or MSE values of the denoised images are nearly same at high threshold values which means that the high threshold values are not much sensitive to the noise present in the image. (d)The performance of the Double Density Dual Tree Wavelet Transform techniques lies between the performance of the rest of the two, that is, Double Density DWT and Double Density DTCWT.

REFERENCES

H. Heartlin Maria, A, Maria Jossy, Analysis of lifting scheme based Double Density Dual-Tree Complex Wavelet Transform for de-noising medical images, Volume 241, September, 2021, Elsevier Publications, https://doi.org/10.1016/j.ijleo.2021.166883

Shyam Lal, Mahesh Chandra, Gopal Krishna Upadhay & Deep Gupta MIT International Journal of Electronics and Communication Engineering Vol. 1, No. 1, Jan. 2011, pp. (8-16) 8 ISSN 2230-7672 ©MIT Publications.

Comparative Study of Dual-Tree Complex Wavelet Transform and Double Density Complex Wavelet Transform for Image Denoising Using Wavelet-Domain International Journal of Scientific and Research Publications, Volume 2, Issue 7, July 2012.

J. Neumann and G. Steidl, ―Dual–tree complex wavelet transform in the frequency domain and an application to signal classification‖, International Journal of Wavelets, Multi resolution and Information Processing IJWMIP, 2004.

I.W. Selesnick, R.G. Baraniuk, and N.G. Kingsbury. The dual-tree complex wavelet transform—A coherent frame work for multiscale signal and image processing. IEEE Signal Processing. Mag., vol. 22, no. 6, pp. 123–151, Nov. 2005.

"The double density DWT," in Wavelets in Signal and Image Analysis: From Theory to Practice, A. Petrosian and F. G. Meyer, Eds. Boston, MA: Kluwer, 2001.

I.W. Selesnick, ―Hilbert transform pairs of wavelet bases. IEEE Signal Process. Letter, vol. 8, no. 6, pp. 170–173 Jun. 2001.

G. Sandhya, K. Kishore―Denoising of Images corrupted by Random noise using Complex Double Density Dual Tree Discrete Wavelet Transform. International Journal of Engineering Research and Applications, vol. 2, Issue 3, pp.079-087, May-Jun 2012

I.W. Selesnick, R.G. Baraniuk, and N.G. Kingsbury, The dual-tree complex wavelet transform—A coherent framework for multiscale signal and image processing. IEEE Signal Processing. Mag., vol. 22, no. 6, pp. 123–151, Nov. 2005.

"Hilbert transform pairs of wavelet bases" IEEE Signal Processing Letter., vol. 8, pp. 170–173, June 2001.

I.W. Selesnick, The double-density dual-tree DWT", IEEE Trans. on Signal Processing, 52(5): pp. 1304-1314, May 2004.

"Image processing with complex wavelets," Phil. Trans. R. Soc. London A, Sept. 1999.